

Invariant morphometric properties of headwater subcatchments

Roger Moussa, François Colin, Michael Rabotin

▶ **To cite this version:**

Roger Moussa, François Colin, Michael Rabotin. Invariant morphometric properties of headwater subcatchments. Water Resources Research, 2011, 47, pp.W08518. 10.1029/2010WR010132 . hal-02647265

HAL Id: hal-02647265
https://hal.inrae.fr/hal-02647265

Submitted on 29 May 2020

HAL is a multi-disciplinary open access archive for the deposit and dissemination of scientific research documents, whether they are published or not. The documents may come from teaching and research institutions in France or abroad, or from public or private research centers.

L'archive ouverte pluridisciplinaire **HAL**, est destinée au dépôt et à la diffusion de documents scientifiques de niveau recherche, publiés ou non, émanant des établissements d'enseignement et de recherche français ou étrangers, des laboratoires publics ou privés.



Distributed under a Creative Commons Attribution - NonCommercial 4.0 International License

Invariant morphometric properties of headwater subcatchments

Roger Moussa,[1] François Colin,[2] and Michaël Rabotin[1]

Received 16 October 2010; revised 18 May 2011; accepted 2 June 2011; published 18 August 2011.

[1] The distinction between the channel network, the headwater subcatchments, and the lateral subcatchments plays an important role in distributed hydrological and ecohydrological applications. This paper presents some newly found invariance properties of headwater and upstream subcatchments and shows that the invariant morphometric properties characterize only natural networks and virtual networks verifying optimal channel networks (OCN) properties but are not verified for virtual non-OCNs. A model based on self-affine properties was developed in order to calculate the number of headwater catchments N and the total upstream area of headwater catchments U as a function of the cutoff area A used to delineate streams. For 18 French catchments between 43 and 116,450 km^2 and for 4 virtual OCNs, results show that $U(A)/A_0$ (with A_0 being the catchment area) is independent of A for $0.5 < A < 5$ km^2 and seems to be constant (0.29 ± 0.03) for various shapes and sizes of channel networks and, consequently, can be considered as an invariant general descriptor of natural channel and virtual OCN networks. On the contrary, this is not the case when the approach is applied on six virtual non-OCNs. Moreover, results show that the knowledge of six morphometric indices enable us to calculate both functions N(A) and U(A) for all values of $A < A_0$. These indices can be considered as geometric and topological properties of headwater and upstream subcatchments and are useful for studying the effects of cutoffs on self-affine river networks or as similarity indices for channel network comparison.

Citation: Moussa, R., F. Colin, and M. Rabotin (2011), Invariant morphometric properties of headwater subcatchments, *Water Resour. Res.*, *47*, W08518, doi:10.1029/2010WR010132.

1. Introduction

[2] The channel network can be seen as the arterial system of the landscape, which controls the spatial and temporal patterns of hydrological, chemical and biotic processes [e.g., *Rinaldo et al.*, 1995, 1998, 2006; *Paola et al.*, 2006; *Convertino et al.*, 2007]. One of the main difficulties in understanding and modeling hydrologic responses is the high spatial complexity of the connectivity between the two independent features: the channel network and subcatchments [*Mesa and Mifflin*, 1986; *Beven and Moore*, 1992; *Robinson et al.*, 1995; *Gurnell and Montgomery*, 1999]. In distributed hydrologic modeling of surface runoff, the connection between subcatchments and the channel network differs whether the subcatchments are upstream or lateral: upstream subcatchments (in darker gray in Figure 1) which can be represented draining directly to, and concentrated at the channel head (in black in Figure 1), while lateral subcatchments (in white in Figure 1) correspond to a right- or a left-bank subcatchment where the exchange can be represented distributed along a reach of the channel network. Therefore, it is a key challenge for hydrology to understand the morphometric properties of both upstream and lateral subcatchments.

[3] Since the pioneer work of *Horton* [1945] and *Strahler* [1957], many different approaches have been developed in order to characterize and differentiate channel network structures (see a synthesis by *Rodríguez-Iturbe and Rinaldo* [1997]) or to identify invariance properties following the recommendation of the *National Research Council* [1991, p. 197] as cited by *Rodríguez-Iturbe et al.* [1992a, p. 1089]: "The search for invariance property across scales as a basic hidden order in hydrologic phenomena, to guide development of specific models and new efforts in measurements is one of the main themes of hydrologic science." During the last 3 decades, digital elevation models (DEMs) were largely used to automatically extract the channel network [e.g., *Montgomery and Dietrich*, 1988, 1989, 1992; *Tarboton et al.*, 1991; *Montgomery and Foufoula-Georgiou*, 1993] (see also recent developments by *Lashermes et al.* [2007], *Passalacqua et al.* [2010], and *Pirotti and Tarolli* [2010] for lidar and high-resolution DEMs), delineate upstream and lateral subcatchments, define the connectivity between the channel network and subcatchments, and calculate the main morphometric properties of the channel network [*Beven and Moore*, 1992; *Gurnell and Montgomery*, 1999]. In the literature, the upstream contributing area (which can be defined on each pixel of the channel network) was largely used as a scale parameter to compute morphometric properties of the channel network (see a synthesis by *Rodríguez-Iturbe and Rinaldo* [1997]). When moving from sources to the catchment outlet, the upstream contributing area corresponds to

[1] INRA, UMR LISAH, Laboratoire d'Étude des Interactions entre Sol-Agrosystème-Hydrosystème, Montpellier, France.
[2] Montpellier SupAgro, UMR LISAH, Laboratoire d'Étude des Interactions entre Sol-Agrosystème-Hydrosystème, Montpellier, France.

Copyright 2011 by the American Geophysical Union.
0043-1397/11/2010WR010132

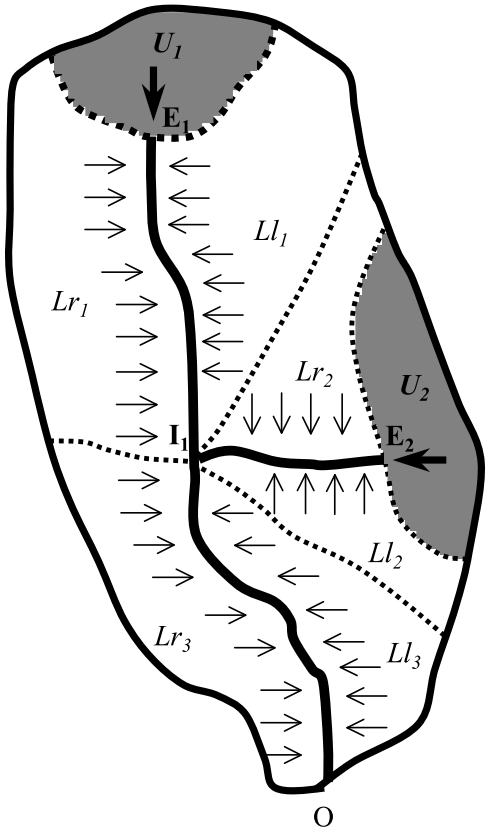


Figure 1. Representation of the connectivity between subcatchments and the channel network, which can be considered to be concentrated at the channel head for upstream subcatchments draining directly to an external node and distributed along the reach for lateral right- and left-bank subcatchments. Channel network encoding is as follows: nodes (external $\mathbf{E_i}$ and internal $\mathbf{I_i}$) are in bold, and reaches and subcatchments (upstream U_i, lateral right-bank Lr_i and lateral left-bank Ll_i) are in italic. The pixels corresponding to the channel network zone are shown in black, and the corresponding upstream subcatchments are in darker gray. The total area of upstream subcatchments is $U = U_1 + U_2$, and the total area of lateral subcatchments is $L = Lr_1 + Lr_2 + Lr_3 + Ll_1 + Ll_2 + Ll_3$.

"channel initiation," to "headwater subcatchments," or more generally to "upstream subcatchments," respectively. While various studies were conducted in the literature in order to characterize each of these entities, very few studies distinguish between upstream and lateral subcatchments.

[4] This distinction between upstream subcatchments (channel initiation, headwater subcatchments or any upstream subcatchment), lateral subcatchments and the channel network, plays an important role in distributed hydrological and ecohydrological applications [*Porporato and Rodríguez-Iturbe*, 2002] because it impacts directly the representation of the catchment topology, and consequently the representation of the process of surface fluxes (water, erosion, pollutant, etc.) exchange between subcatchments and the channel network [*Woolhiser et al.*, 1990; *Vertessy et al.*, 1993; *Fortin et al.*, 2001; *Moussa et al.*, 2002, 2007a, 2007b; *Moussa*, 2008b]. Hence, the catchment area A_0 can be considered as the sum of the total area of upstream subcatchments (noted U), the total area of lateral subcatchments (noted L) and the total area of the channel network (noted C)

$$U + L + C = A_0. \quad (1)$$

While in the literature the morphometric properties of the upstream contributing area were largely studied [*Rodríguez-Iturbe and Rinaldo*, 1997; *Moussa*, 1997b], few papers studied the number, the total area of upstream subcatchments and their spatial distribution within a catchment. Therefore, it is important to elucidate what are the morphometric properties of U, L and C within a catchment and for various shapes, scales and sizes of catchments.

[5] This paper aims to present some newly found invariance properties of upstream and lateral subcatchments, and aims to analyze if these new invariant morphometric properties characterize all topological structure of networks, or only natural channel networks and virtual networks verifying optimal channel networks (OCN) properties [*Rinaldo et al.*, 1992; *Rigon et al.*, 1993]. The paper is structured in three sections. First, we present the state of the art. Second, we present the heuristic approach used to study the morphometric properties of both upstream and lateral subcatchments on the basis of similarity properties of channel networks [*Rodríguez-Iturbe and Rinaldo*, 1997; *Paola et al.*, 2006]. Finally, applications were conducted on 28 natural and virtual (OCN and non-OCN) networks in order to validate (or not) the approach on various shapes and sizes of natural and virtual channel networks.

2. Invariant Morphometric Properties of the Channel Network: State of the Art

[6] The methodology used herein is based on the analysis of the properties of the upstream contributing area and distinguish between upstream and lateral subcatchments. This section presents first the algorithms to extract the channel network, upstream subcatchments, and lateral subcatchments from DEMs and then discusses morphometric properties of the upstream drained area on some main nodes of the channel network.

2.1. Extraction of Upstream and Lateral Subcatchments From DEMs

[7] DEMs are generally used to automatically extract the channel network and delineate upstream and lateral subcatchments. The common method used is the D8 approach which assigns a pointer from each cell to one of its eight neighbors, in the direction of the steepest downward slope [*O'Callaghan and Marks*, 1984; *Band*, 1986] (Figure 2a) and calculates the contributing draining area on each pixel (Figure 2b). The D8 method has also been improved by the D∞ multiple-flow direction method [*Tarboton*, 1997], the multiple-flow method [*Quinn et al.*, 1991], the D8-LAD (least angular deviation) and D8-LTD (least transversal deviation) method [*Orlandini et al.*, 2003]. All these methods mitigate some disadvantages of the D8 method but introduce new disadvantages as expressed by *Tarboton* [1997] and *Orlandini et al.* [2003]. In particular, multiple drainage directions produce numerical dispersion of area from a DEM cell to all neighboring cells with a lower elevation. In this respect, nondispersive methods using a single drainage direction (such as D8, D8-LAD, and D8-LTD) appear

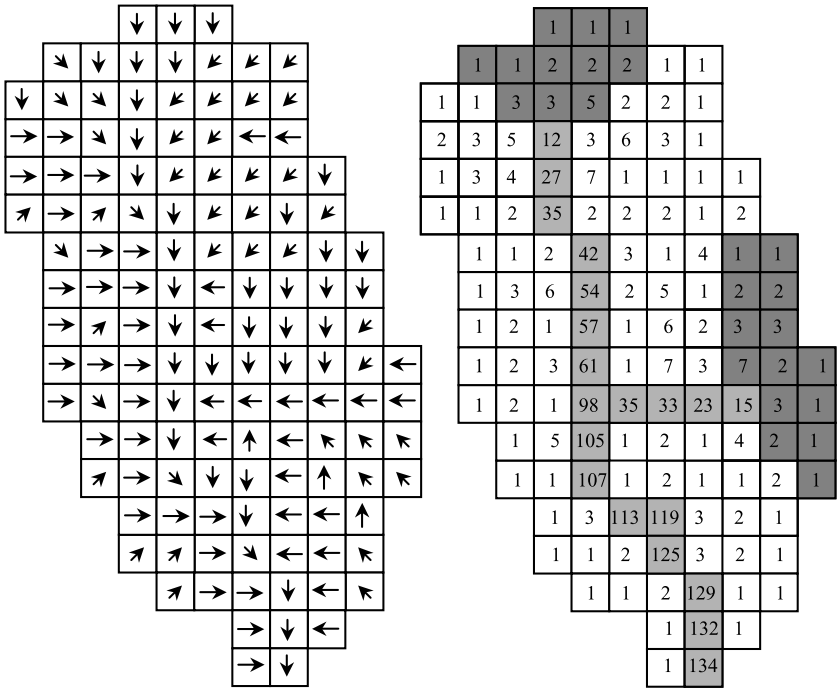


Figure 2. (a) Identification of the drainage direction of each pixel from a digital elevation model (DEM). (b) Contributing drainage area (number of pixels) at each pixel of the catchment. The channel network extracted with an upstream cutoff area A = 10 pixels is shown in lighter gray, and the corresponding upstream subcatchments is in darker gray.

preferable because they produce convergent river networks with single thread (nonbraided) channels consistent with the physical representation of rivers at the scale studied in this paper.

[8] In order to characterize the morphometric properties of the upstream and lateral subcatchments at various scales, the methodology applied herein consists on analyzing the channel network properties for various values of $A < A_0$. The use of constant cutoff area A appears an essential requirement when assuming that network-forming discharges can be surrogated by total contributing area [*Rodríguez-Iturbe et al.*, 1992a]. For each value of A, there will be a corresponding topology of the channel network, as shown in Figure 3. For low values of A (e.g., 0.1 to 10 km^2 in the French context [*Moussa*, 1991; *Le Moine*, 2008, pp. 293–322]), the channel network extracted can be compared to blue lines on geographic maps, and the resulting basin subdivision into headwater and lateral subcatchments can be used for distributed hydrological modeling applications [*Fortin et al.*, 2001; *Moussa et al.*, 2002, 2007a]. For large values of A (e.g., A > 10 km^2), the resulting basin subdivision can be used for semidistributed hydrological modeling applications under a limited consideration of spatial heterogeneity of hydrological characteristics within a river basin [e.g., *Diskin and Simpson*, 1978; *Schumann*, 1993; *Hughes and Sami*, 1994; *Moussa*, 1997a; *Moussa et al.*, 2007a, 2007b]; in this case, the determination of the number and the size of subcatchments should be determined in relation to the spatial correlation scale of the forcing (typically rainfall) field that drives the model. In all cases, the objective herein when using a constant cutoff area A is not to extract the exact channel network and to identify channel heads, but to use the upstream contributing area A as a scale criteria in order to characterize the morphometric properties of upstream and lateral subcatchments. Consequently U, L and C can be considered as a function of A, and equation (1) can be written

$$U(A) + L(A) + C(A) = A_0. \quad (2)$$

2.2. Universal Power Laws

[9] The analysis of U(A), L(A), and C(A) as a function of A can be undertaken using similarity properties of the channel network. The statistical similarity properties of the planar structure of channel networks was extensively studied since the pioneer works of *Horton* [1932, 1945] and *Strahler* [1952, 1957]. After *Mandelbrot*'s [1983] work, the last 20 years have seen a revolution in the range of quantitative tools to characterize the physical structures of channel networks [*Rinaldo et al.*, 1991, 1993; *Paola et al.*, 2006; *Moussa*, 2009] (see a synthesis by *Rodríguez-Iturbe and Rinaldo* [1997]). Under the assumption that network-forming discharges can be surrogated by total contributing area, *Rodríguez-Iturbe et al.* [1992a] have shown that the distribution of mass (contributing drainage area at any point of the channel network; Figure 2b) is a power law form such as

$$P[A_t \geq A] = kA^{-\beta}, \quad (3)$$

where $P[A_t \geq A]$ is the probability that the contributing drainage area A_t be higher or equal to a given area A and k and β are two parameters. It is important to notice that often the exponent β is statistically indistinguishable

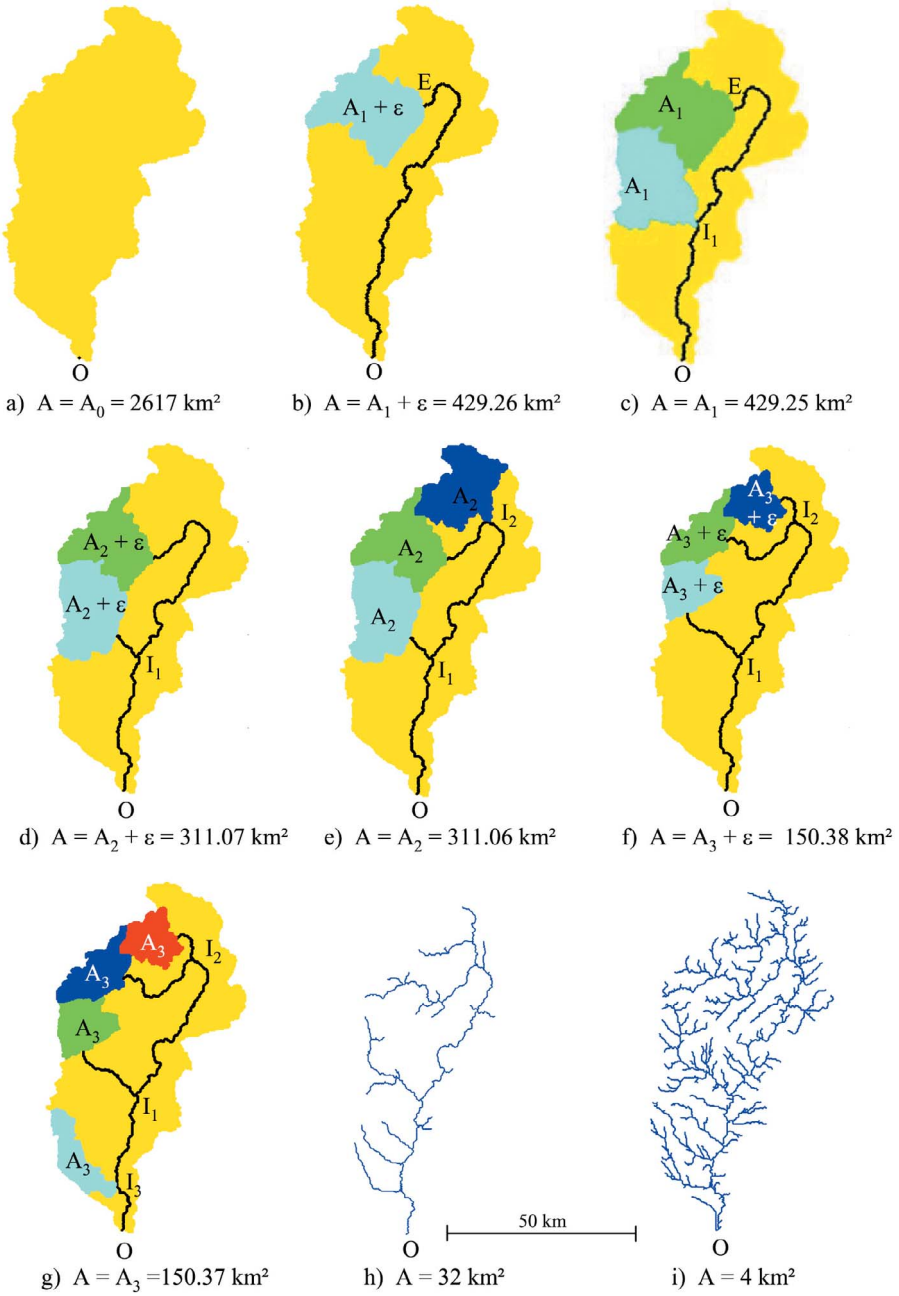


Figure 3. Example of the channel network of the Hérault catchment extracted for various values of the cutoff area A.

among different basins, is unaffected by the size of the support cutoff area used to identify the network, and is approximately equal to 0.43 ± 0.02. The recurrence of a similar values of β suggests some resemblance to a self-organized critical phenomenon, as described by *Bak et al.* [1988, 1989] where a spatially extended dissipative dynamical system naturally evolves into states with no characteristic time or length scales [*Rodríguez-Iturbe and Rinaldo*, 1997]. Moreover, *Rodríguez-Iturbe et al.* [1992b] and *Rinaldo et al.* [1992] have suggested new local and global optimality principles (optimal channel networks, OCN) linking energy dissipation and runoff production with the three-dimensional structure of the river basins. OCN configurations are obtained by minimizing the total rate of energy expenditure $\sum_i A_i^{0.5}$ where A_i is the contributing drainage area at a pixel i of the channel network [*Rigon et al.*, 1993]. *Rodríguez-Iturbe and Rinaldo* [1997] have shown that the exponent β is generally close to 0.43 for OCN channel networks, while β differs largely from 0.43 for non-OCN networks [e.g., *Maritan et al.*, 1996; *Rigon et al.*, 1996, 1998]. *Rodríguez-Iturbe et al.*'s [1992a, 1992b] and *Rinaldo et al.*'s [1992] results are an important character of seemingly general nature, that is, regardless of size, vegetation, geology, soil, climate, or orientation of the catchment, and their theory explains the most important structural characteristics observed in the geomorphology of drainage systems. The universal power law distribution suggested by *Rodríguez-Iturbe et al.* [1992a, 1992b] characterizes the whole structure of the channel network, and

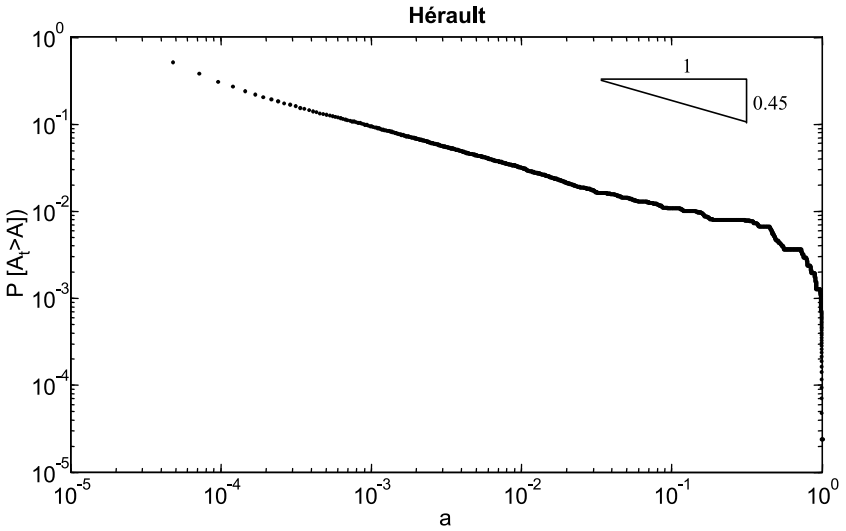


Figure 4. Cumulative distribution of the drained area as a function of the relative support threshold area for the Hérault catchment.

in the literature, little attention was paid to the spatial distribution of subcatchments inside a catchment, and to the distinction between upstream and lateral subcatchments.

2.3. Identification of the Main Nodes of the Channel Network

[10] Upstream and lateral subcatchments are connected either to the source nodes or to the reaches of the channel network. The geometry of the channel network can be characterized by the relative position of the nodes, the area drained by each node, and the distance from each node to the outlet. We distinguish three types of nodes, the outlet node (denoted O), the external nodes (denoted E) or channel tip draining upstream subcatchments, and the internal nodes (denoted I) draining either lateral right- or left-bank subcatchments (Figure 1).

[11] The methodology used herein is based on the procedure proposed by *Moussa* [2008a, 2008b]. For a fixed A, let N(A) be the number of external nodes corresponding to the number of upstream subcatchments. Figure 3 shows the evolution of the channel network topology for various values of $A < A_0$ for the Hérault catchment ($A_0 = 2617$ km^2). For $A = A_0$ (Figure 3a), there is no channel network and the catchment is considered as a single upstream catchment. When A decreases $A < A_0$ (Figure 3b), the catchment has only one upstream subcatchment (N = 1). We define the threshold A_1 such that the total number of external nodes varies from N = 1 (for $A = A_1 + \varepsilon$, the term ε being the area of one pixel; Figure 3b) to N = 2 (for $A = A_1$; Figure 3c). For $A = A_1$, the first internal node I_1 of the channel network appears, and the channel network has two external nodes. When A decreases from A_1 to A_2 ($A_2 \leq A < A_1$) as in Figures 3c and 3d, the channel network has two upstream subcatchments, and three reaches linked each one to a lateral right- and left-bank subcatchments. We define the threshold A_2 such that the total number of external nodes varies from N = 2 (for $A = A_2 + \varepsilon$; Figure 3d) to N = 3 (for $A = A_2$; Figure 3e). For $A = A_2$, the second internal node I_2 appears, and the channel network has three external nodes. The procedure continues iteratively, and in the step "i," the internal node I_i corresponding to a threshold area A_i appears and the channel network has (i + 1) external nodes. In the particular case where each internal node has only two entry reaches, we have

$$A_i = \max(A \text{ for } A < A_0), \tag{4}$$

such that $N(A_i) = i + 1$. We observe that the structure of the channel network becomes more complex when A decreases from $A = A_0$ to $A = 4$ km^2 as in Figures 3h and 3i.

[12] Section 3 aims to couple the methodology presented above and the power law properties in order to study the morphometric properties of both upstream and lateral subcatchments for various values of the cutoff area A.

3. Morphometric Properties of Upstream and Lateral Subcatchments

[13] This section analyzes the relationships between U(A), L(A) and C(A) and their variation as a function of A. In order to nondimensionalize equation (2), let $a = A/A_0$ (with $0 < a \leq 1$), $n(a) = N(A)$, $u(a) = U(A)/A_0$, $l(a) = L(A)/A_0$ and $c(a) = C(A)/A_0$ with

$$u(a) + l(a) + c(a) = 1. \tag{5}$$

3.1. Main Relationships

[14] The function $C(A) = c(a)A_0$ represents the total area of the pixels draining an area higher than A. Hence, the function c(a) represents the probability that a pixel drains an area higher than A and can be obtained from equation (3) when applied on the whole set of pixels within a catchment

$$c(a) = P[A_t \geq A] = kA^{-\beta}. \tag{6}$$

Figure 4 shows the cumulative distribution of the drained area of all the pixels of the Hérault catchment. We observe that $\beta \approx 0.45$ (with $k \approx 0.0037$ for a 250 m DEM resolution) is of the same range of the universal value 0.43 ± 0.02

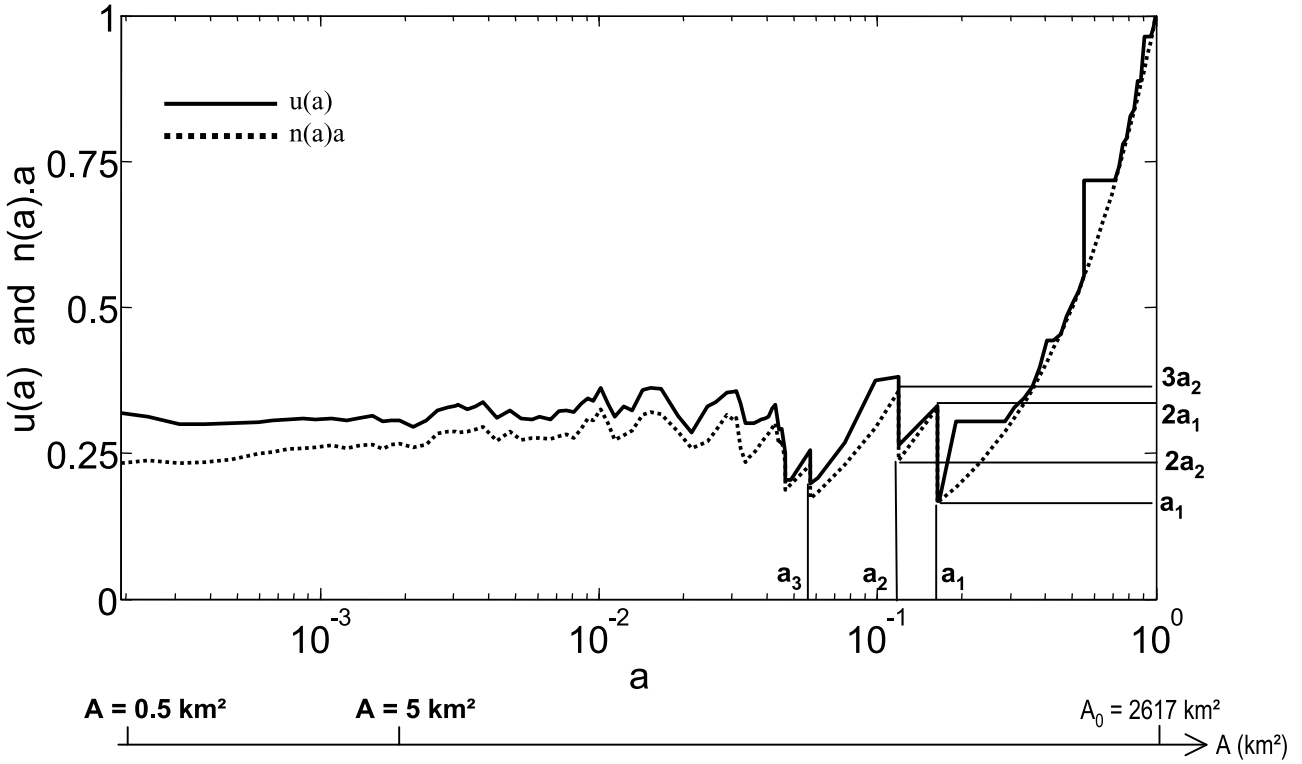


Figure 5. Relationship between the relative upstream drained area $a = A/A_0$, the total area of upstream subcatchments u(a) (solid line), and the function n(a)a (dotted line), where n(a) is the total number of upstream subcatchments.

obtained by various authors [*Rodríguez-Iturbe and Rinaldo*, 1997]. By combining equations (5) and (6) we obtain

$$u(a) + l(a) = 1 - kA^{-\beta}. \quad (7)$$

From equation (7) we observe that the knowledge of u(a) enables us to calculate l(a). Even if u(a) can be approximated by n(a)a, the function u(a) is higher or equal and not strictly equal to n(a)a because each of the N(A) upstream subcatchments in Figure 2b drains an area higher or equal to A. In the example in Figure 2b (where the total area A_0 = 134 pixels) and for three values of A = 9, 10, and 11 pixels, the number of source subcatchments remains constant N(A) = 2, the total area of source subcatchments also remains constant U(A) = 25 pixels (and hence u(a) = 25/134 = 0.187), while the product NA = 18, 20, and 22 pixels, respectively, and hence na = 0.134, 0.149, and 0.164, respectively. Therefore, for a given threshold area A, we have

$$U(A) \geq N(A)A \;\Rightarrow\; u(a) \geq n(a)a. \quad (8)$$

Section 3.2 analyzes the properties of the two functions u(a) and n(a)a, and discusses the correlation between them.

3.2. Properties of Upstream Subcatchments

[15] Figure 5 shows the effects of varying the threshold area ratio a on the two functions u(a) and n(a)a for the example of the Hérault catchment, for which a_1 = 0.1640, a_2 = 0.1189, and a_3 = 0.0575. The function u(a) decreases from u(a) = 1 for a = 1 (Figure 3a) to $u(a) = a_1$ for $a = a_1 + \varepsilon$ (ε being the area of one pixel; Figure 3b). When a decreases from $a_1 + \varepsilon$ to a_1, u(a) increases drastically from a_1 to approximately $2a_1$ because the number of upstream subcatchments jumps from 1 to 2 (Figures 3b and 3c). Then, when a decreases from a_1 to $a_2 + \varepsilon$, u(a) decreases from approximately $2a_1$ to approximately $2a_2$, etc. More generally, u(a) is a switchback function such that u(a) decreases when a decreases from a_i to a_{i+1} with

$$u(a_i + \varepsilon) \approx ia_i, \quad u(a_i) \approx (i+1)a_i. \quad (9)$$

When a_i decreases, equation (9) tends to $u(a_i + \varepsilon) \approx u(a_i)$. For $a < a_3$, we observe that both u(a) and n(a)a are fairly constant when A decreases (e.g., A < 50 km^2 in Figure 5).

[16] Let $\overline{u}_t$ and $\overline{na}_t$ be the mean values of u(a) and n(a)a, respectively, calculated for low values of A, such that $A_{min} < A < A_{max}$, where A_{min} and A_{max} are the minimum and maximum values, respectively, of A such that u(a) and n(a)a are fairly constant. The choice of A_{min} is guided by the number of pixels of the cutoff area as a function of the resolution of the DEM (Δx) because the user has to fix a minimum number of pixels in order to reduce the uncertainty on the calculation of the upstream drained area. The cutoff area A_{max} has to be chosen such that u(a) and n(a)a remain constant on the interval $[A_{min}, A_{max}]$. For the applications on French catchments, we choose 0.5 km^2 < A < 5 km^2 because this range of values of A corresponds to the range of upstream area drained by headwater subcatchments on the majority of French subcatchments [*Le Moine*, 2008]; note that the choice of A_{min} = 0.5 km^2 (which corresponds to 89 pixels if Δx = 75 m and 16 pixels if Δx = 250 m) can be reduced especially if high-resolution DEMs are available, and the value of A_{max} can be extended, for example, to

Table 1. Effects of the D8 and D8-LTD Algorithms and Digital Elevation Model Resolution Δx Used for Channel Network Extraction on the Main Morphometric Properties of Upstream and Lateral Subcatchments on the Hérault Basin[a]

Algorithm	Δx (m)	A_0 (km^2)	$a_1 = A_1/A_0$	$a_2 = A_2/A_0$	$a_3 = A_3/A_0$	$\overline{u}_t$	$\overline{na}_t$	α	k	β
D8	75	2629	0.156	0.117	0.056	0.303	0.263	1.15	0.0012	0.456
D8	150	2634	0.163	0.122	0.056	0.312	0.276	1.13	0.0024	0.452
D8	200	2760	0.152	0.132	0.057	0.313	0.274	1.14	0.0031	0.450
D8	250	2619	0.164	0.112	0.058	0.307	0.269	1.14	0.0037	0.451
D8	300	2759	0.169	0.114	0.062	0.310	0.268	1.15	0.0046	0.439
D8-LTD	75	2627	0.156	0.117	0.056	0.307	0.269	1.13	0.0012	0.453
D8-LTD	150	2637	0.160	0.118	0.060	0.318	0.279	1.14	0.0023	0.448
D8-LTD	200	2617	0.158	0.118	0.056	0.311	0.272	1.14	0.0032	0.455
D8-LTD	250	2633	0.161	0.117	0.059	0.311	0.268	1.16	0.0036	0.449
D8-LTD	300	2654	0.159	0.117	0.057	0.309	0.268	1.15	0.0047	0.442

[a]The morphometric properties are the three relative thresholds, a_1, a_2, and a_3; the mean values of u(a) (denoted $\overline{u}_t$) and n(a)a (denoted $\overline{na}_t$) for 0.5 km^2 < A < 5 km^2; the ratio $\alpha = \overline{u}_t/\overline{na}_t$; and the two adjusted parameters k and β of the power law.

50 km^2, as shown in Figure 5. However, even if the values of A_{min} and A_{max} are slightly modified, the values of $\overline{u}_t$ and $\overline{na}_t$ remains approximately similar. We obtain for the Hérault catchment (Figure 5), $\overline{u}_t \approx 0.303$ and $\overline{na}_t \approx 0.263$ with $\overline{u}_t/\overline{na}_t \approx 1.15$. Thus, we can establish a simple empirical relationship such as

$$\overline{u}_t = \alpha\,\overline{na}_t, \tag{10}$$

where α is an empirical parameter that describes the ratio $\alpha = \overline{u}_t/\overline{na}_t$. Hence, for low values of a (e.g., a < 0.02 or A < 50 km^2 in Figure 5), the function u(a) can be approximated by the function αn(a)a. In the example of Figure 5, we verify that u(a) is higher or equal to u(a)a, and the comparison of the two functions u(a) and αn(a)a (for a < 0.02 and $\alpha \approx 1.15$) give a Nash-Sutcliffe efficiency criteria of 0.98.

[17] In order to analyze the sensitivity of the procedure to the algorithm used to extract the channel network from DEM, and to the DEM resolution Δx, two algorithms (D8 using the algorithm presented by *Moussa and Bocquillon* [1994] and the D8-LTD from *Orlandini et al.* [2003]) and five resolutions of the DEM were considered Δx = 75, 150, 200, 250, and 300 m. Table 1 shows the main results obtained for the Hérault catchment. We observe that both D8 and D8-LTD algorithms gave comparable results for all studied variables, A_0, a_1, a_2, a_3, $\overline{u}_t$, $\overline{na}_t$, α, k, and β. In the following, we choose the D8 algorithm because it is simple and largely available in Geographical Information Systems. We also observe that the parameter k increases when Δx

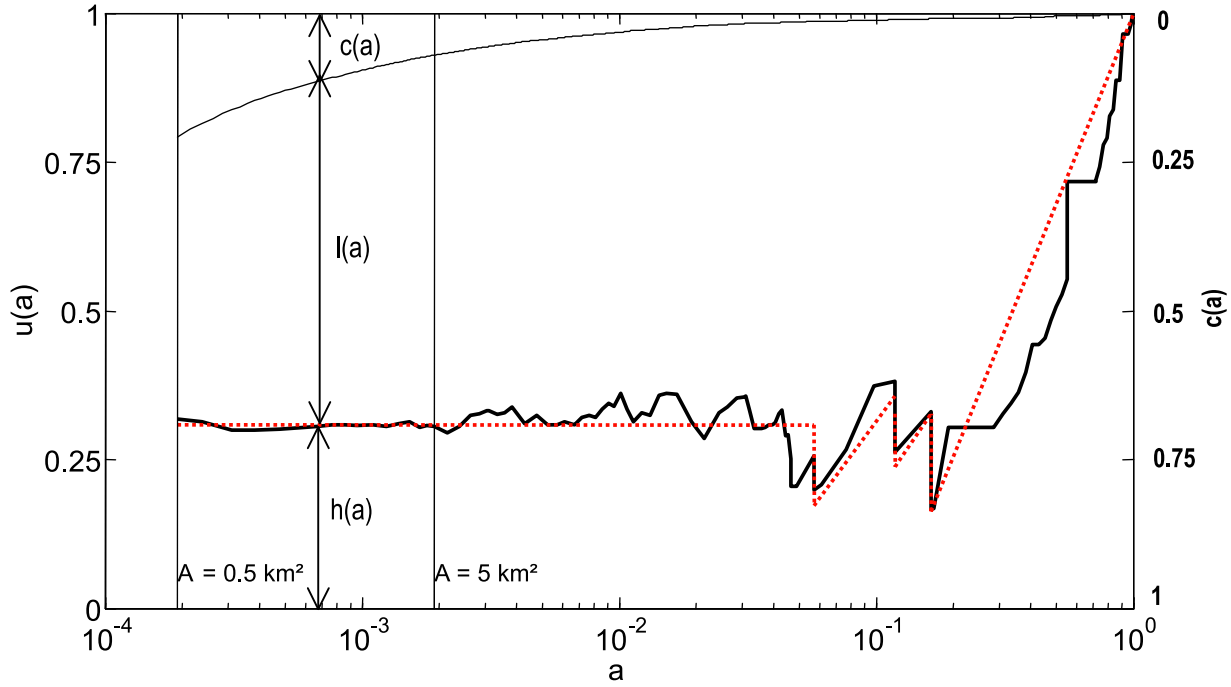


Figure 6. Morphometric properties of upstream and lateral subcatchments of the Hérault catchment as a function of a = A/A_0. The left *y* axis shows the relationship between the total area of upstream subcatchments u(a) obtained from a DEM (thick solid line) and the simulated value from equation (12) (dotted line). The right *y* axis shows the total area of the pixels of the channel network c(a) obtained from equation (6) (thin solid line). The vertical dashed lines indicate the location of A = 0.5 km^2 and 5 km^2.

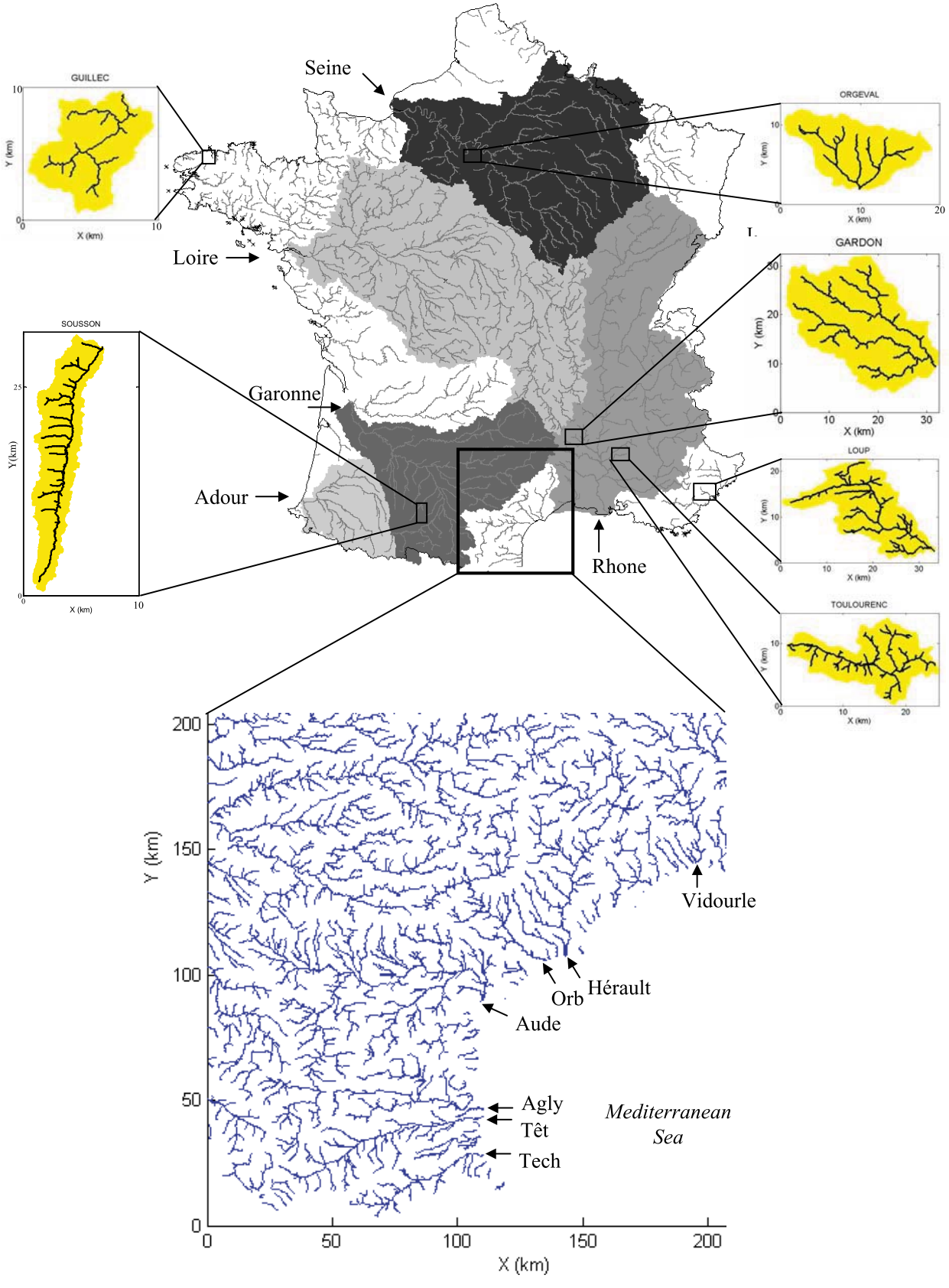


Figure 7. Location of the 18 French catchments used in this study. The coordinates (latitude and longitude, respectively) of the left bottom corner are France (48°50′N, 02°20′E), Languedoc-Roussillon region, southern France, with in order from the Spanish border: Tech, Têt, Agly, Aude, Orb, Hérault, and Vidourle (43°30′N, 03°54′E), Guillec (48°39N, 04°21′W), Sousson (43°30′N, 0°26′E), Orgeval (48°54N, 1°58′E), Gardons (44°30′N, 4°15′E), Loup (43°42′N, 7°03′E), and Toulourenc (44°10′N, 5°09′E).

Table 2. Main Characteristics and Nondimensionalized Descriptors of the Studied Catchments[a]

Basin	S_0 (km^2)	$s_1 = S_1/S_0$	$s_2 = S_2/S_0$	$s_3 = S_3/S_0$	$\overline{h}_t$	$\overline{ns}_t$	$\alpha = \overline{h}_t/\overline{ns}_t$	k	β
Tech	738	0.073	0.066	0.065	0.312	0.255	1.22	0.0077	0.451
Têt	1,356	0.085	0.069	0.066	0.293	0.239	1.23	0.0051	0.476
Agly	1,101	0.331	0.237	0.061	0.315	0.256	1.23	0.0077	0.416
Aude	5,346	0.169	0.120	0.048	0.302	0.245	1.23	0.0024	0.476
Orb	1582	0.164	0.083	0.079	0.306	0.251	1.22	0.0059	0.421
Hérault	2,617	0.164	0.119	0.057	0.303	0.263	1.15	0.0037	0.462
Vidourle	860	0.131	0.108	0.101	0.311	0.251	1.24	0.0073	0.445
Gardon	523	0.469	0.168	0.137	0.308	0.251	1.23	0.0102	0.406
Orgeval	104	0.419	0.135	0.095	0.324	0.274	1.18	0.0044	0.498
Guillec	42	0.244	0.206	0.066	0.323	0.273	1.18	0.0070	0.470
Toulourenc	158	0.162	0.110	0.109	0.321	0.274	1.17	0.0045	0.433
Loup	293	0.107	0.104	0.079	0.304	0.261	1.17	0.0032	0.480
Sousson	118	0.066	0.049	0.037	0.226	0.204	1.11	0.0048	0.440
Loire	117,778	0.180	0.177	0.123	0.260	0.206	1.26	0.0008	0.481
Rhône	91,323	0.148	0.135	0.101	0.262	0.203	1.29	0.0007	0.461
Seine	87,245	0.230	0.226	0.157	0.296	0.228	1.29	0.0008	0.491
Garonne	56,391	0.185	0.157	0.053	0.250	0.205	1.22	0.0010	0.469
Adour	16,893	0.255	0.172	0.123	0.248	0.192	1.29	0.0015	0.487

[a]The characteristics are catchment area A_0; the three relative thresholds, a_1, a_2, and a_3; the mean values of u(a) (denoted $\overline{u}_t$) and n(a)a (denoted $\overline{na}_t$) for 0.5 km^2 < A < 5 km^2; the ratio $\alpha = \overline{u}_t/\overline{na}_t$; and the two adjusted parameters k and β of the power law.

increases while the values of the three nondimensionalized descriptors a_1, a_2, and a_3 (and hence the threshold areas A_1, A_2, and A_3) and the values of $\overline{u}_t$, $\overline{na}_t$, and β remain approximately constant for all values of Δx. The parameter k depends on the DEM resolution Δx and k increases quasi-linearly with Δx; a small departure from linearity in this relationship is likely related to the sinuosity of the channels which has fractal properties [*Tarboton et al.*, 1990; *Helmlinger et al.*, 1993].

3.3. Properties of Lateral Subcatchments

[18] The nondimensionalized total area of lateral subcatchments can be obtained from equation (7)

$$l(a) = 1 - kA^{-\beta} - u(a). \tag{11}$$

The function u(a) can be represented empirically using the following relationships: (1) For $a_1 < a \le 1$, u(a) is approximated by a linear decrease from u = 1 for a = 1 to u = a_1 for $a = a_1 + \varepsilon$. (2) For $a_3 < a \le a_1$, u(a) is a switchback function that is approximated by two linear relationships: $u(a) = 2a_1$ for $a = a_1$, $u(a) = 2a_2$ for $a = a_2$ and $u(a) = 3a_2$ for $a = a_2$, $u(a) = 3a_3$ for $a = a_3$. (3) For $a_n < a \le a_3$, u(a) is approximated by a constant value $\overline{u}_t$ (with $a_n = 0.5/A_0$ corresponding to the minimum value of the cutoff area A = 0.5 km^2).

[19] As a first approximation we obtain

$$\begin{aligned} u(a) &= a, \quad a_1 < a \le 1, \\ u(a) &= 2a, \quad a_2 < a \le a_1, \\ u(a) &= 3a, \quad a_3 < a \le a_2, \\ u(a) &= \overline{u}_t, \quad a_n < a \le a_3. \end{aligned} \tag{12}$$

[20] Figure 6 shows the good agreement of u(a) obtained from the analysis of DEMs, and the function calculated from equation (12) with a Nash-Sutcliffe criteria equal to 0.97. Consequently, the knowledge of the six parameters a_1, a_2, a_3, $\overline{u}_t$, k, and β enables us to calculate all three functions u(a), l(a), and c(a) when using equations (6), (11), and (12), as shown in Figure 6.

4. Application

4.1. Study Sites

[21] In order to validate (or not) the approach on various catchments' shapes and sizes, we apply equations (6), (11), and (12) on natural and virtual catchments. Eighteen French catchments are used in the applications (Figure 7 and Table 2): seven are located in the Languedoc-Roussillon region southern France and have their outlets in the Mediterranean Sea (in order from the Spanish border: Tech, Têt, Agly, Aude, Orb, Hérault, and Vidourle), one is a tributary of the Rhone (Gardon d'Anduze), one is located in the Parisian zone (Orgeval), one is located in Brittany western France (Guillec), two are located in southeastern France (Toulourenc and Loup), one is located southwestern France (Sousson), and the five main French rivers (Loire, Rhone, Seine, Garonne, and Adour). The catchments' areas cover large spatial scales and range between 42 km^2 (Guillec) and 116,500 km^2 (Loire). Then, the same methodology was applied on virtual OCN and non-OCN channel networks in order to study if the invariant properties are verified for OCN or not [*Rodríguez-Iturbe et al.*, 1992b; *Rinaldo et al.*, 1992; *Rigon et al.*, 1993]. The virtual channel networks were chosen from *Rodríguez-Iturbe and Rinaldo* [1997]: the spiral pattern, the *Peano* [1890] catchment, four virtual non-OCN catchments, denoted virtual 1 to virtual 4 [*Rodríguez-Iturbe and Rinaldo*, 1997, p. 270], and four virtual OCN catchments, denoted virtual 5 to virtual 8 [*Rodríguez-Iturbe and Rinaldo*, 1997, p. 272], as shown in Figure 8. Note that the OCN catchments virtual 5, virtual 6, virtual 7, and virtual 8 were developed from the initial conditions of the non-OCN catchments virtual 1, virtual 2, virtual 3, and virtual 4, respectively, as stated by *Rodríguez-Iturbe and Rinaldo* [1997, pp. 267–277].

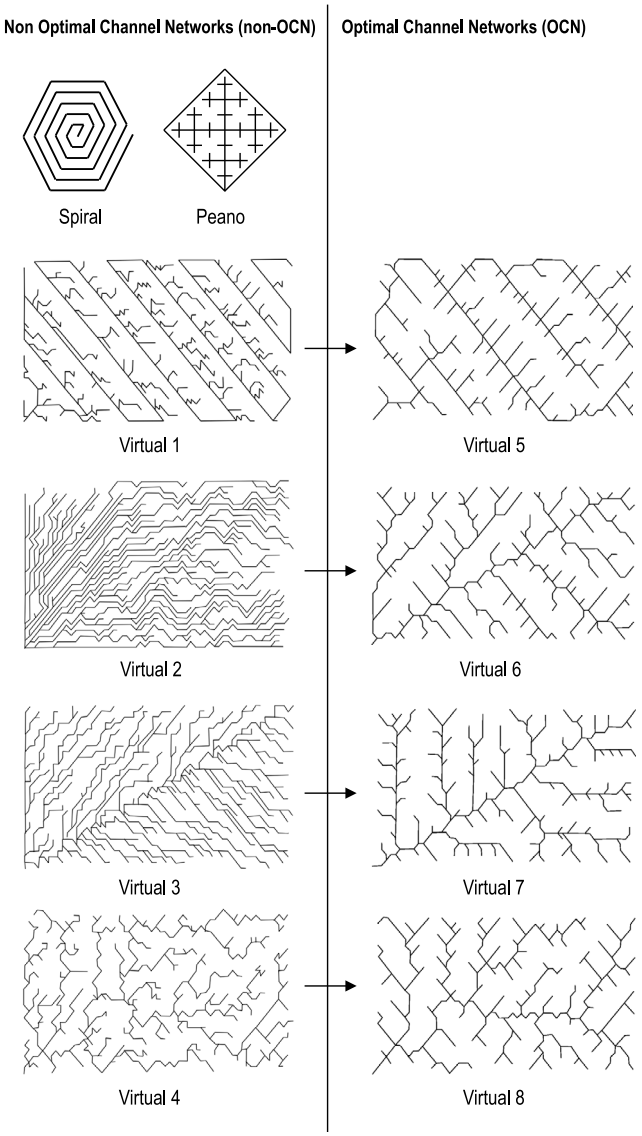


Figure 8. Ten patterns of virtual networks. (left) Six patterns of virtual nonoptimal channel networks: the spiral, the Peano, and four virtual networks, denoted virtual 1 to virtual 4 [from *Rodríguez-Iturbe and Rinaldo*, 1997, p. 270]. (right) Four patterns of virtual optimal channel networks (OCNs), denoted virtual 5 to virtual 8 [from *Rodríguez-Iturbe and Rinaldo*, 1997, p. 272]. The OCNs virtual 5, virtual 6, virtual 7, and virtual 8 were developed from the initial conditions of the non-OCN catchments virtual 1, virtual 2, virtual 3, and virtual 4, respectively, as stated by *Rodríguez-Iturbe and Rinaldo* [1997, pp. 267–277].

4.2. Case of Natural Channel Networks

[22] The DEMs are in the form of the French National Geographic Institute (IGN) blocks and have a 75 m grid resolution. High-resolution DEMs derived by lidar are now widely available and enable us to recognize in detail the hillslope to valley transition morphology [*Tarolli and Dalla Fontana*, 2009] and channel network extraction [*Lashermes et al.*, 2007; *Passalacqua et al.*, 2010; *Pirotti and Tarolli*, 2010]; however, for the goals of this paper and for regional analysis approaches a coarse DEM is enough to derive scaling relations and statistical analysis on channel network and subcatchments. In the applications, the flow directions are identified from DEM using the D8 method, then we analyze the morphometric properties of the channel network and upstream and lateral subcatchments for various values of A.

[23] Table 2 shows the values of the nondimensionalized indices $a_1 = A_1/A_0$, $a_2 = A_2/A_0$, and $a_3 = A_3/A_0$ (with $0 < a_3 < a_2 < a_1 \leq 0.5$) for the 18 French catchments. We observe that a_1 covers a large range of variations from approximately 0.07 for elongated basins (e.g., Tech, Têt, and Sousson) to 0.47 for channel networks where the internal node I_1 is located near the outlet (e.g., Gardon and Orgeval). Table 2 also shows the values of $\overline{u}_t$, $\overline{na}_t$, α, k, and β, and Figure 9 shows examples of eight catchments for the relationships u(a) and c(a). For all studied catchments, the constant β of the universal power law remains constant and equal to 0.43 ± 0.04. The value $\overline{u}_t$ calculated for 0.5 km^2 < A < 5 km^2 varies slightly between 0.25 (e.g., Garonne) and 0.32 (e.g., Orgeval and Guillec) and can be estimated equal to 0.294 ± 0.031 for all 18 catchments. The mean value $\overline{na}_t$ calculated for 0.5 km^2 < A < 5 km^2 varies between 0.19 (e.g., Adour) and 0.27 (e.g., Orgeval, Guillec, and Toulourenc) and can be estimated equal to 0.242 ± 0.030 for all 18 catchments. The ratio α varies between 1.11 (e.g., Sousson) and 1.29 (e.g., Rhone, Seine, and Adour) and can be estimated equal to 1.22 ± 0.08. Hence, the values of $\overline{u}_t$ and $\overline{na}_t$ seems to be constant for various channel networks' shapes and sizes and consequently can be considered as invariant general descriptors of natural catchment networks.

4.3. Case of Optimal Channel Networks and Nonoptimal Channel Networks

[24] The aim of the application on virtual networks is to study if the two invariant properties $\overline{u}_t$ and $\overline{na}_t$ also characterize (or not) OCNs and/or non-OCNs. The 10 virtual catchments in Figure 8 were digitalized and computed into a GIS software. For each catchment, a virtual DEM was created using an algorithm derived from AGREE procedure (F. L. Hellweger, AGREE—DEM Surface Reconditioning System, http://www.ce.utexas.edu/prof/maidment/gishydro/ferdi/research/agree/agree.html). The procedure consists of creating a plane, and the elevation of the cells corresponding to each virtual network is lowered; the procedure is repeated on each subcatchment until a proper DEM is made. Then, we use the same algorithm as for natural networks, and we limit the analysis for a cutoff area A_{min} fixed equal to 89 pixels as for natural catchments (which corresponds to A_{min} = 0.5 km^2 for Δx = 75 m).

[25] The morphometric properties of the six non-OCN catchments in Figure 8 (left) were largely studied in the literature, and results have shown that β differs largely from the value 0.43 which is the constant generally obtained for natural channel networks. However, non-OCNs can evolve to OCNs as in the examples of virtual 1–4 (Figure 8, left) which evolve to virtual 5–8 (Figure 8, right), with β close to 0.43 as for OCNs [*Rodríguez-Iturbe and Rinaldo*, 1997, pp. 251–355].

[26] Figure 10 (left) shows the relationships u(a), c(a), and n(a)a as a function of the threshold a for the six non-OCNs in Figure 8 (left). For all six virtual non-OCN, and for low values of a, the two functions u(a) and n(a)a tends to decrease for low values of a, which is not the case for natural channel

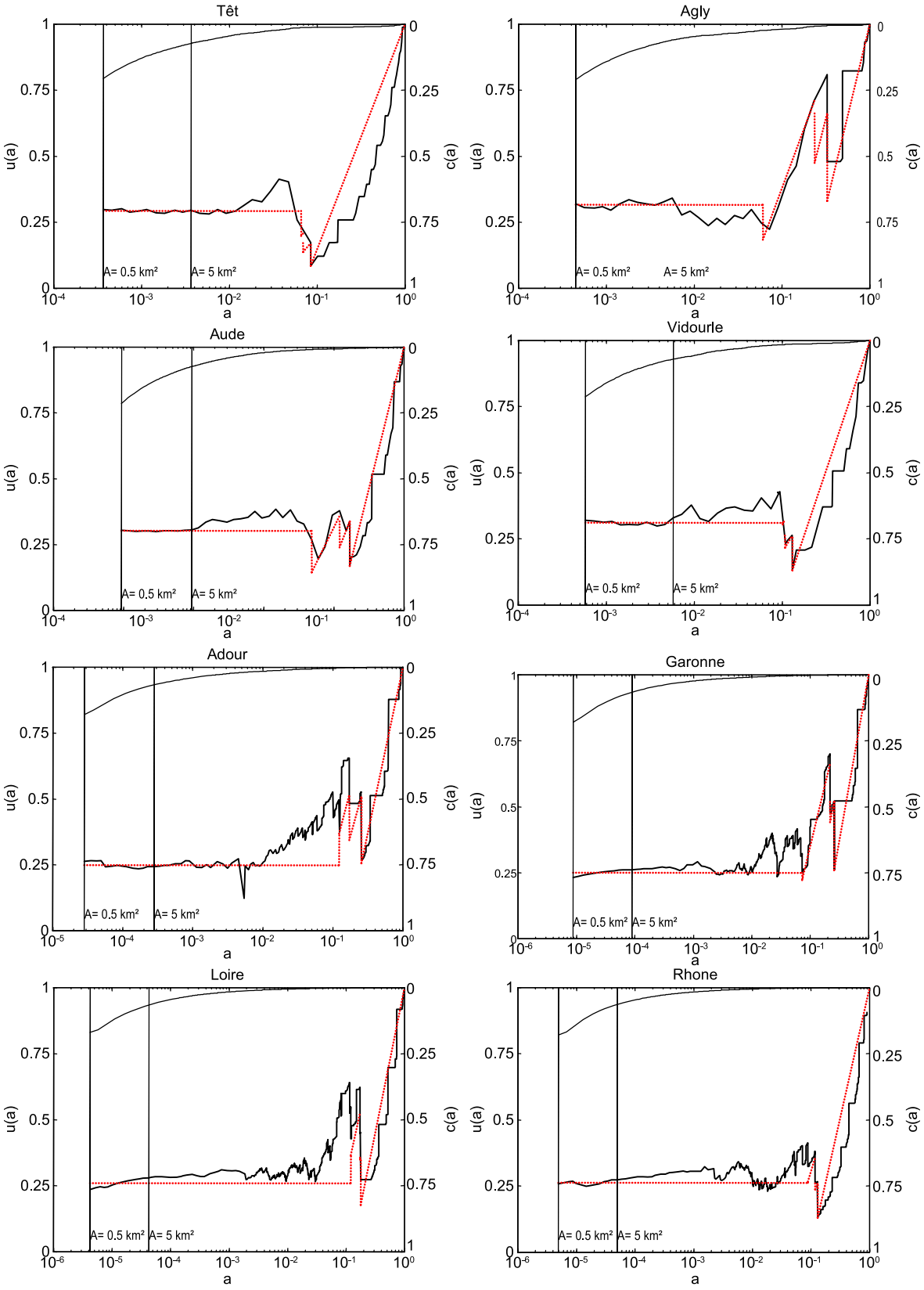


Figure 9. Examples of morphometric properties of upstream and lateral subcatchments of eight catchments (Têt, Agly, Aude, Vidourle, Adour, Garonne, Loire, and Rhone) as a function of $a = A/A_0$. The left *y* axis shows the relationship between the relative total area of upstream subcatchments u(a) obtained from a DEM (thick solid line) and the simulated value from equation (12) (dotted line). The right *y* axis shows the relative total area of the pixels of the channel network c(a) obtained from equation (6) (thin solid line). The vertical dashed lines indicate the location of A = 0.5 and 5 km^2.

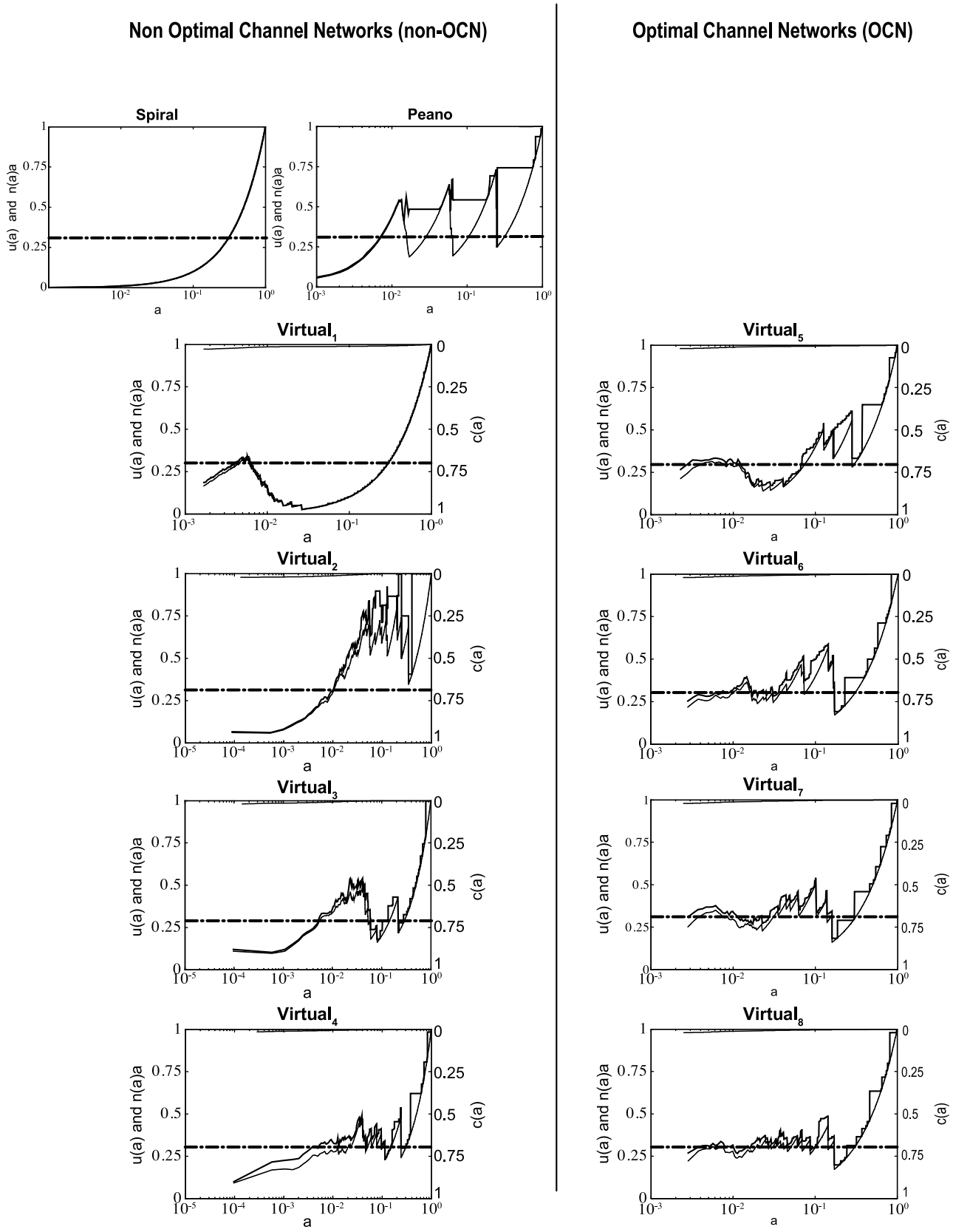


Figure 10. Morphometric properties of upstream and lateral subcatchments of the 10 virtual channel networks of Figure 8. The left *y* axis shows the relative total area of upstream subcatchments u(a) (solid line) and the function n(a)a (dotted line), where n(a) is the total number of upstream subcatchments. The right-axis shows the relative total area of the pixels of the channel network c(a) (solid line). The horizontal dash-dotted line indicates the value $\overline{u}_t = 0.29$ obtained for natural networks.

networks for which u(a) and n(a)a tend to a constant value. Moreover, in some cases (e.g., spiral and virtual 1), we do not observe switchback functions. We distinguish three cases. First, for the spiral pattern and all elongated non-OCN, u(a) and n(a)a tend to zero when a decreases. Second, for the Peano network, we observe a trifurcation recursive geometric structure which leads to a similar result with u(a) and n(a)a tending to zero when a decreases. Third, for the remaining four virtual networks, we observe that u(a) and n(a)a tend to a constant ranging between 0.05 and 0.1 which is largely inferior to the values 0.22–0.32 obtained for natural channels; the main reason is that the channel network is structured as a set of parallel elongated channels linked to the main channel network as in the case of the examples of virtual networks 2 and 3 or around a trifurcation node as for virtual networks 2 and 4.

[27] Figure 10 (right) shows the relationships u(a), c(a), and n(a)a as a function of the threshold a for the four virtual OCNs in Figure 8 (right). For the four virtual OCNs (virtual 5–8), we observe that when a decreases, u(a) and n(a)a tend to a constant ranging between 0.22 and 0.32 which corresponds to the values obtained for natural channels.

[28] Hence, the descriptors β, $\overline{u}_t$, and $\overline{na}_t$ seem to be invariant and independent of the value of a for natural and virtual OCN channel networks. However, this is not the case for virtual non-OCN channel networks where $\overline{u}_t$ and $\overline{na}_t$ are not invariant and depend on the value of a.

4.4. Discussion

[29] An empirical model using six parameters a_1, a_2, a_3, $\overline{u}_t$, k, and β was developed to calculate the three functions U(A), L(A), and C(A) for all range of $A < A_0$ (equations (6), (11), and (12)). In the discussion, we distinguish two cases according to the range of variation of A.

[30] First, we study the case of low values of A, as for example $0.5 < A < 5$ km^2 for the applications herein where the channel network extracted from DEMs can be compared to blue lines in the French geologic and climatic context. The two invariant descriptors $\overline{u}_t$ and $\overline{na}_t$ can be used to approximate the total area and the number of headwater subcatchments when extracted with a constant cutoff area A. To the question, "when the channel network is extracted using a cutoff area A, what is the total area of headwater subcatchments"?, the response is that the total area of headwater subcatchments for natural catchments can be considered for a large number of natural catchments as independent of A, and is equal to approximately $U(A) = (0.29 \pm 0.03)\, A_0$. For the example of the Hérault catchment ($A_0 = 2617$ km^2), we can approximate the total area of headwater subcatchments $U(A) = 759 \pm 79$ km^2 for all values of A. This also means that the total number of headwater subcatchments can be approximated by $N(A) = (0.24 \pm 0.03)\, A_0/A$ with approximately N equal to 1256 ± 157, 628 ± 78, and 157 ± 20 for A equal to 0.5, 1, and 4 km^2, respectively.

[31] Second, for larger values of $A < A_0$, we distinguish two cases according to the value of A: 5 km$^2 < A < A_3$ and $A_3 < A < A_0$. For 5 km$^2 < A < A_3$, the results obtained above for $0.5 < A < 5$ km^2, can be extended in some cases for all values of $A < A_3$ (e.g., $A_3 = 149$ km^2 for the Hérault). Hence, in the example of the Hérault catchment, the total number of upstream subcatchments can be approximated by N equal to 63 ± 8, 13 ± 2, and 6 ± 1 for A equal to 10, 50, and 100 km^2, respectively. These properties can be helpful for the estimation of the number and the total area of all upstream subcatchments draining an area equal to A, for characterizing the number of subcatchments of the same area within a catchment, or for choosing the location of outlets for experimentation. For $A_3 < A < A_0$, we have shown that the function U(A) has a switchback shape (equation (12)), and is discontinuous around the values of $A = A_1$, A_2 and A_3. The values of a_1, a_2, and a_3 (corresponding to A_1, A_2, and A_3, respectively) are independent of the grid size (Table 1), can be considered as descriptors of the channel network topology and connectivity, and can be classified by order: a_1, a_2, and a_3.

[32] Finally, for both cases studied above, these invariant properties of headwater (or upstream) subcatchments can be used to characterize lateral subcatchments. Equation (2) shows that the total area of lateral subcatchments $L(A) = A_0 - U(A) - C(A)$. The function C(A) representing the total area of the pixels of the channel network can be calculated from the universal power law $C(A) = kA^{-\beta}A_0$ [*Rodríguez-Iturbe et al.*, 1992a]. While β is invariant and independent of the grid size, the parameter k depends on the grid size of the DEM. Hence, the knowledge of U(A) enables the calculation of L(A) as a function of the cutoff area A. While C(A) and L(A) depend on the value of A, the sum $L(A) + C(A) = A_0 - H(A)$ is independent of the value of A when $0.5 < A < 5$ km^2 because U(A) can be considered independent from the value of A. In conclusion, all three functions U(A), L(A) and C(A) can be calculated as a function of the six parameters a_1, a_2, a_3, $\overline{u}_t$, k, and β. While the parameters a_1, a_2, a_3, and k differ according to the channel network shape, the two parameters $\overline{u}_t$ and β can be considered invariant for all natural channel networks and virtual networks verifying OCN properties.

5. Conclusion

[33] The catchment topological structure is determined from the interconnection between the channel network and subcatchments which are either upstream or lateral subcatchments. The distinction between upstream and lateral subcatchments plays an important role in representing the connections with the channel network.

[34] For a large range of French natural channel networks across scales (e.g., 18 French catchments between 43 and 116,450 km^2, this paper verifies that the constant β of the universal power law is constant and equal to 0.43 ± 0.04 [*Rodríguez-Iturbe et al.*, 1992a], and shows that the total area of headwater subcatchments $U(A) = \overline{u}_t A_0$ (where $\overline{u}_t$ is invariant and equal to 0.29 ± 0.03), is constant and independent of the value of the cutoff area A when $0.5 < A < 5$ km^2 and in some cases this invariant property is verified below a scale where the channel network is resolved to include about 4 or more source nodes ($A < A_3$). Moreover, the total number of source catchment N(A) can be approximated as a function of A using a simple empirical relationship such as $NA = \overline{na}_t A_0$, where $\overline{na}_t$ is invariant and equal to 0.24 ± 0.03 for all studied channel networks. The results show also that $\overline{u}_t$ and $\overline{na}_t$ are independent of the DEM resolution, remain similar for all catchments, and the ratio $\alpha = \overline{u}_t/\overline{na}_t$ seems to be constant and equal to 1.22 ± 0.08. In comparison to the constant β of the universal power law, both invariant descriptors $\overline{u}_t$ and $\overline{na}_t$ can be considered

as universal descriptors of natural channel networks and virtual OCNs. However, this is not the case for non-OCNs where $\overline{u}_t$ and $\overline{na}_t$ are not invariant and depend on the value of a.

[35] Finally, the knowledge of the six parameters a_1, a_2, a_3, $\overline{u}_t$, k, and β enables us to calculate all three functions U(A), L(A) and C(A). The values of a_1, a_2, and a_3 are independent of the grid size and can be classified by order of importance: a_1, a_2, and a_3. While $\overline{u}_t$ and β are relatively constant for all channel networks, the parameters a_1, a_2, a_3, and k differ according to the channel network shape. These indices can be considered as geometric and topological properties of both upstream and lateral subcatchments and are useful for studying the effects of cutoffs on self-affine river networks, for controlling the characteristics of both natural and virtual channel networks, for modeling the topology of river networks using the morphometric properties of cutoffs, or as similarity indices for channel network comparison and regionalization on poorly gauged catchments [e.g., *Blöschl and Sivapalan*, 1995; *Aryal et al.*, 2002; *Sivapalan et al.*, 2003; *Blöschl*, 2005].

[36] **Acknowledgments.** We thank Stefano Orlandini and Giovanni Moretti (University of Modena and Reggio Emilia, Italy) for providing us with the D8-LTD algorithm. We thank the associate editor and the anonymous reviewers for insightful comments that considerably improved the manuscript. This research was supported by the French National Institute of Agricultural Research (INRA), Montpellier SupAgro, and by the French National Hydrological Programme (PNRH) of the French Ministry of Research.

References

Aryal, S. K., E. M. O'Loughlin, and R. G. Mein (2002), A similarity approach to predict landscape saturation in catchments, *Water Resour. Res.*, *38*(10), 1208, doi:10.1029/2001WR000864.

Bak, P., C. Tang, and K. Wiesenfeld (1988), Self-organized criticality, *Phys. Rev. A*, *38*(1), 364–374, doi:10.1103/PhysRevA.38.364.

Bak, P., K. Chen, and M. Creutz (1989), Self-organized criticality in the 'Game of Life,' *Nature*, *342*, 780–782, doi:10.1038/342780a0.

Band, L. E. (1986), Topographic partition of watersheds with digital elevation models, *Water Resour. Res.*, *22*(1), 15–24, doi:10.1029/WR022i001p00015.

Beven, K. J., and I. D. Moore (1992), *Terrain Analysis and Distributed Modelling in Hydrology*, 249 pp., John Wiley, Chichester, U. K.

Blöschl, G. (2005), Rainfall-runoff modeling of ungauged catchments, in *Encyclopedia of Hydrological Sciences*, edited by M. G. Anderson, vol. 3, pp. 2061–2079, John Wiley, Chichester, U. K.

Blöschl, G., and M. Sivapalan (1995), Scale issues in hydrological modeling—A review, *Hydrol. Processes*, *9*, 251–290, doi:10.1002/hyp.3360090305.

Convertino, M., R. Rigon, A. Maritan, I. Rodriguez-Iturbe, and A. Rinaldo (2007), Probabilistic structure of the distance between tributaries of given size in river networks, *Water Resour. Res.*, *43*, W11418, doi:10.1029/2007WR006176.

Diskin, M. H., and E. S. Simpson (1978), A quasi linear spatially distributed model for the surface runoff systems, *Water Resour. Bull.*, *14*, 903–918.

Fortin, J. P., R. Turcotte, S. Massicotte, R. Moussa, and J. Fitzback (2001), Distributed watershed model compatible with remote sensing and GIS data. I: Description of the model, *J. Hydrol. Eng.*, *6*, 91–99, doi:10.1061/(ASCE)1084-0699(2001)6:2(91).

Gurnell, A. M., and A. R. Montgomery (1999), *Hydrological Applications of GIS*, 176 pp., John Wiley, Chichester, U. K.

Helmlinger, K. R., P. Kumar, and E. Foufoula-Georgiou (1993), On the use of digital elevation model data for Hortonian and fractal analyses of channel networks, *Water Resour. Res.*, *29*, 2599–2613, doi:10.1029/93WR00545.

Horton, R. E. (1932), Drainage-basin characteristics, *Eos Trans. AGU*, *13*, 350.

Horton, R. E. (1945), Erosional development of streams and their drainage basins; hydrophysical approach to quantitative morphology, *Geol. Soc. Am. Bull.*, *56*, 275–370, doi:10.1130/0016-7606(1945)56[275:EDOSAT]2.0.CO;2.

Hughes, D. A., and K. Sami (1994), A semi-distributed, variable-time interval model of catchment hydrology—Structure and parameter estimation procedures, *J. Hydrol.*, *155*, 265–291, doi:10.1016/0022-1694(94)90169-4.

Lashermes, B., E. Foufoula-Georgiou, and W. Dietrich (2007), Channel network extraction from high resolution topography using wavelets, *Geophys. Res. Lett.*, *34*, L23S04, doi:10.1029/2007GL031140.

Le Moine, N. (2008), Le bassin versant de surface vu par le souterrain: Une voie d'amélioration des performances et du réalisme des modèles pluie-débit?, Ph.D. thesis, 262 pp., Univ. Pierre et Marie Curie, Paris.

Mandelbrot, B. B. (1983), *The Fractal Geometry of Nature*, 468 pp., W. H. Freeman, New York.

Maritan, A., A. Rinaldo, I. Rodríguez-Iturbe, R. Rigon, and A. Giacometti (1996), Scaling in river networks, *Phys. Rev. E*, *53*, 1510–1515, doi:10.1103/PhysRevE.53.1510.

Mesa, O. J., and E. R. Mifflin (1986), On the relative role of hillslope and network geometry in hydrologic response, in *Scale Problems in Hydrology*, edited by V. K. Gupta, I. Rodríguez-Iturbe, and E. F. Wood, chap. 1, pp. 1–17, D. Reidel, Norwell, Mass.

Montgomery, D. R., and W. E. Dietrich (1988), Where do channels begin?, *Nature*, *336*, 232–234.

Montgomery, D. R., and W. E. Dietrich (1989), Source areas, drainage density, and channel initiation, *Water Resour. Res.*, *25*, 1907–1918, doi:10.1029/WR025i008p01907.

Montgomery, D. R., and W. E. Dietrich (1992), Channel initiation and the problem of landscape scale, *Science*, *255*, 826–830, doi:10.1126/science.255.5046.826.

Montgomery, D. R., and E. Foufoula-Georgiou (1993), Channel network source representation using digital elevation models, *Water Resour. Res.*, *29*, 3925–3934, doi:10.1029/93WR02463.

Moussa, R. (1991), Variabilité spatio-temporelle et modélisation hydrologique. Application au bassin du Gardon d'Anduze, Ph.D. thesis, 314 pp., Univ. of Montpellier II Sci. et Tech. du Languedoc, Montpellier, France.

Moussa, R. (1997a), Geomorphological transfer function calculated from digital elevation models for distributed hydrological modelling, *Hydrol. Processes*, *11*, 429–449, doi:10.1002/(SICI)1099-1085(199704)11:5<429::AID-HYP471>3.0.CO;2-J.

Moussa, R. (1997b), Is the drainage network a fractal Sierpinski space?, *Water Resour. Res.*, *33*, 2399–2408, doi:10.1029/97WR01899.

Moussa, R. (2008a), Effect of channel network topology, basin segmentation and rainfall spatial distribution on the GIUH transfer function, *Hydrol. Processes*, *22*, 395–419, doi:10.1002/hyp.6612.

Moussa, R. (2008b), What controls the width function shape, and can it be used for channel network comparison and regionalization?, *Water Resour. Res.*, *44*, W08456, doi:10.1029/2007WR006118.

Moussa, R. (2009), Definition of new equivalent indices of Horton-Strahler ratios for the derivation of the Geomorphological Instantaneous Unit Hydrograph, *Water Resour. Res.*, *45*, W09406, doi:10.1029/2008WR007330.

Moussa, R., and C. Bocquillon (1994), TraPhyC-BV: A hydrologic information system, *Environ. Software*, *9*(4), 217–226, doi:10.1016/0266-9838(94)90020-5.

Moussa, R., M. Voltz, and P. Andrieux (2002), Effects of the spatial organization of agricultural management on the hydrological behaviour of a farmed catchment during flood events, *Hydrol. Processes*, *16*, 393–412, doi:10.1002/hyp.333.

Moussa, R., N. Chahinian, and C. Bocquillon (2007a), Distributed hydrological modelling of a Mediterranean mountainous catchment—Model construction and multi-site validation, *J. Hydrol.*, *337*, 35–51, doi:10.1016/j.jhydrol.2007.01.028.

Moussa, R., N. Chahinian, and C. Bocquillon (2007b), Erratum to "Distributed hydrological modelling of a Mediterranean mountainous catchment—Model construction and multi-site validation," [*J. Hydrol. 337*(2007) 35–51], *J. Hydrol.*, *345*, 254, doi:10.1016/j.jhydrol.2007.08.012.

National Research Council (1991), *Opportunities in the Hydrologic Sciences*, Natl. Acad. Press, Washington, D. C.

O'Callaghan, J. F., and D. M. Marks (1984), The extraction of drainage networks from digital elevation data, *Comput. Vision Graphics Image Process.*, *28*, 323–344, doi:10.1016/S0734-189X(84)80011-0.

Orlandini, S., G. Moretti, M. Franchini, B. Aldighieri, and B. Testa (2003), Path-based methods for the determination of nondispersive drainage

directions in grid-based digital elevation models, *Water Resour. Res.*, *39*(6), 1144, doi:10.1029/2002WR001639.

Paola, C., E. Foufoula-Georgiou, W. E. Dietrich, M. Hondzo, D. Mohrig, G. Parker, M. E. Power, I. Rodríguez-Iturbe, V. Voller, and P. Wilcock (2006), Toward a unified science of the Earth's surface: Opportunities for synthesis among hydrology, geomorphology, geochemistry, and ecology, *Water Resour. Res.*, *42*, W03S10, doi:10.1029/2005WR004336.

Passalacqua, P., P. Tarolli, and E. Foufoula-Georgiou (2010), Testing space-scale methodologies for automatic geomorphic feature extraction from lidar in a complex mountainous landscape, *Water Resour. Res.*, *46*, W11535, doi:10.1029/2009WR008812.

Peano, G. (1890), Sur une courbe qui remplit toute une aire plane, *Math. Ann.*, *36*, 157–160, doi:10.1007/BF01199438.

Pirotti, F., and P. Tarolli (2010), Suitability of lidar point density and derived landform curvature maps for channel network extraction, *Hydrol. Processes*, *24*, 1187–1197, doi:10.1002/hyp.7582.

Porporato, A., and I. Rodríguez-Iturbe (2002), Ecohydrology—A challenging multidisciplinary research perspective, *Hydrol. Sci. J.*, *47*(5), 811–821, doi:10.1080/02626660209492985.

Quinn, P., K. Beven, P. Chevallier, and O. Planchon (1991), The prediction of hillslope flow paths for distributed hydrological modeling using digital terrain models, *Hydrol. Processes*, *5*, 59–79, doi:10.1002/hyp.3360050106.

Rigon, R., I. Rodríguez-Iturbe, and E. Ijjasz-Vasquez (1993), Optimal channel networks: A framework for the study of river basin morphology, *Water Resour. Res.*, *29*, 1635–1646, doi:10.1029/92WR02985.

Rigon, R., I. Rodríguez-Iturbe, A. Maritan, A. Giacometti, D. G. Tarboton, and A. Rinaldo (1996), On Hack's law, *Water Resour. Res.*, *32*, 3367–3374, doi:10.1029/96WR02397.

Rigon, R., I. Rodríguez-Iturbe, and A. Rinaldo (1998), Feasible optimality implies Hack's law, *Water Resour. Res.*, *34*, 3181–3189, doi:10.1029/98WR02287.

Rinaldo, A., A. Marani, and R. Rigon (1991), Geomorphological dispersion, *Water Resour. Res.*, *27*(4), 513–525, doi:10.1029/90WR02501.

Rinaldo, A., I. Rodríguez-Iturbe, R. Rigon, R. L. Bras, E. Ijjasz-Vasquez, and A. Marani (1992), Minimum energy and fractal structure of drainage networks, *Water Resour. Res.*, *28*, 2183–2195, doi:10.1029/92WR00801.

Rinaldo, A., I. Rodríguez-Iturbe, R. Rigon, E. Ijjasz-Vazquez, and R. L. Bras (1993), Self-organized fractal river networks, *Phys. Rev. Lett.*, *70*, 822–825, doi:10.1103/PhysRevLett.70.822.

Rinaldo, A., G. K. Vogel, R. Rigon, and I. Rodríguez-Iturbe (1995), Can one gauge the shape of a basin?, *Water Resour. Res.*, *31*, 1119–1127, doi:10.1029/94WR03290.

Rinaldo, A., I. Rodríguez-Iturbe, and R. Rigon (1998), Channel networks, *Annu. Rev. Earth Planet. Sci.*, *26*, 289–327, doi:10.1146/annurev.earth.26.1.289.

Rinaldo, R., J. R. Banavar, and A. Maritan (2006), Trees, networks, and hydrology, *Water Resour. Res.*, *42*, W06D07, doi:10.1029/2005WR004108.

Robinson, J. S., M. Sivapalan, and J. D. Snell (1995), On the relative roles of hillslope processes, channel routing, and network geomorphology in the hydrologic response of natural catchments, *Water Resour. Res.*, *31*, 3089–3101, doi:10.1029/95WR01948.

Rodríguez-Iturbe, I., and A. Rinaldo (1997), *Fractal River Basins: Chance and Self-Organization*, 547 pp., Cambridge Univ. Press, New York.

Rodríguez-Iturbe, I., E. Ijjasz-Vasquez, R. L. Bras, and D. G. Tarboton (1992a), Power-law distribution of mass and energy in river basins, *Water Resour. Res.*, *28*, 1089–1093, doi:10.1029/91WR03033.

Rodríguez-Iturbe, I., A. Rinaldo, R. Rigon, R. L. Bras, and E. Ijjasz-Vasquez (1992b), Energy dissipation, runoff production and the three-dimensional structure of channel networks, *Water Resour. Res.*, *28*, 1095–1103, doi:10.1029/91WR03034.

Schumann, A. H. (1993), Development of conceptual semi-distributed models and estimation of their parameters with the aid of GIS, *Hydrol. Sci. J.*, *38*(6), 519–528, doi:10.1080/02626669309492702.

Sivapalan, M., et al. (2003), IAHS decade on predictions in ungauged basins (PUB), 2003–2012: Shaping an exciting future for the hydrological sciences, *Hydrol. Sci. J.*, *48*(6), 857–880, doi:10.1623/hysj.48.6.857.51421.

Strahler, A. N. (1952), Hypsometric (area altitude) analysis of erosional topography, *Geol. Soc. Am. Bull.*, *63*, 1117–1142, doi:10.1130/0016-7606(1952)63[1117:HAAOET]2.0.CO;2.

Strahler, A. N. (1957), Quantitative analysis of watershed geomorphology, *Eos Trans. AGU*, *38*, 912.

Tarboton, D. G. (1997), A new method for the determination of flow directions and upslope areas in grid digital elevation models, *Water Resour. Res.*, *33*, 309–319, doi:10.1029/96WR03137.

Tarboton, D. G., R. L. Bras, and I. Rodriguez-Iturbe (1990), Comment on "On the fractal dimension of stream networks" by Paolo La Barbera and Renzo Rosso, *Water Resour. Res.*, *26*, 2243–2244, doi:10.1029/WR026i009p02243.

Tarboton, D. G., R. L. Bras, and I. Rodríguez-Iturbe (1991), On the extraction of channel networks from digital elevation models, *Hydrol. Processes*, *5*, 81–100, doi:10.1002/hyp.3360050107.

Tarolli, P., and G. Dalla Fontana (2009), Hillslope-to-valley transition morphology: New opportunities from high resolution DTMs, *Geomorphology*, *113*, 47–56, doi:10.1016/j.geomorph.2009.02.006.

Vertessy, R. A., T. J. Hatton, P. J. O. O'Shaughnessy, and M. D. A. Jayasuriya (1993), Predicting water yield from a mountain ash forest catchment using a terrain analysis based catchment model, *J. Hydrol.*, *150*, 665–700, doi:10.1016/0022-1694(93)90131-R.

Woolhiser, D. A., R. E. Smith, and D. C. Goodrich (1990), KINEROS, a kinematic runoff and erosion model: Documentation and user manual, *Rep. ARS-77*, Agric. Res. Serv., U.S. Dep. of Agric., Washington, D. C.

F. Colin, Montpellier SupAgro, UMR LISAH, Laboratoire d'Étude des Interactions entre Sol-Agrosystème-Hydrosystème, 2 Place Pierre Viala, F-34060 Montpellier CEDEX 1, France.

R. Moussa and M. Rabotin, INRA, UMR LISAH, Laboratoire d'Étude des Interactions entre Sol-Agrosystème-Hydrosystème, 2 Place Pierre Viala, F-34060 Montpellier CEDEX 1, France. (moussa@supagro.inra.fr)